

Chapter 13

Climate Change Impacts on Some Hydrological Variables in the Zayandeh-Rud River Basin, Iran

Saeid Eslamian, Hamid R. Safavi, Alireza Gohari, Mahdi Sajjadi, Vahid Raghbi, and Mohammad Javad Zareian

13.1 Introduction

Global warming has significant impacts on the various systems like agriculture (Bates et al. 2008), environment (Dawson and Spannagle 2009), the hydrologic cycle (Douville et al. 2002) and the urban water supply (Barnett et al. 2005; Betts 2005). Based on comprehensive reports by the Intergovernmental Panel on Climate Change (IPCC), which is done in continental scale, global warming has the effects not only on the global temperature; but also causes changes in performance of the systems which have interaction with atmosphere. Widespread impacts of climate change on the earth's climate systems have been detected by the IPCC assessments in the past periods (Fakhri et al. 2012a), including: Impact on atmosphere (e.g. change in frequency and intensity of precipitation, change in wind speed, change in atmospheric and cloud water vapour, change in the El Nino phenomenon, Monsoon, change in extreme events like flood and drought); Impact on hydrosphere (e.g. change in runoff quantity and quality, change in groundwater quantity and quality, rising global average sea level, saltwater penetration into groundwater in coastal areas); Impact on cryosphere (e.g. change in the amount of ice in the earth, change in the amount of existing glaciers, change in earth's snow cover); and impact on biosphere (e.g. change in vegetation type, change in water requirement and performance of crops, change in earth wildlife and change in the amount of erosion) (Gohari et al. 2013). Undoubtedly, human activities would increase in the future, and consequently the amount of greenhouse gases emission will increase, leading to intensified changes in global climate variables (Eslamian et al. 2011).

Atmosphere-ocean general circulation models (AOGCM) are the most reliable tools currently available for the projection of the global climate system responses

S. Eslamian • H.R. Safavi (✉) • A. Gohari • M. Sajjadi • V. Raghbi • M.J. Zareian
Department of Civil Engineering, Isfahan University of Technology, Isfahan, Iran
e-mail: hasafavi@cc.iut.ac.ir

under climate change (IPCC 2007). There are three type of uncertainties sources in the usage of AOGCMs at climate change impacts assessments including: the uncertainties in future greenhouse gas and aerosol emissions (Parry et al. 2004), the uncertainties in AOGCMs (Khan et al. 2006) and the uncertainties in global climate model sensitivities (Elmahdi 2008). Ignoring these uncertainties reduces the credibility of the final results and presents the unreal results for decision-makers (Prudhomme et al. 2003). Multiple climate change scenarios produced by different AOGCMs have been used to better represent and deal with uncertainties (Tao et al. 2009; Tao and Zhang 2010; Daccache et al. 2011). This study aims to evaluate the climate change impact assessment on the climate variables such as maximum temperature, minimum temperature, mean temperature and precipitation of the Zayandeh-Rud basin in Central Iran). A probabilistic ensemble model approach was used to project the climate change impacts in the study area. This ecosystem along mountain slopes is closely stacked because of sharp vertical temperature and precipitation gradients and is particularly sensitive to anthropogenic climatic change (Diaz et al. 2003; Huber et al. 2005; Bradley et al. 2006; Nogués-Bravo et al. 2007; Sorg et al. 2012). An innovate approach used to regionalize projected series in station scale to improve the reliability of the climate change impact assessment.

13.2 Zayandeh-Rud River Basin

The semi-arid Zayandeh-Rud River Basin is one of the most strategic river basins of Iran (Madani and Marino 2009). This river basin with an area of 26,917 km² is located in central Iran, between the 50° 24' to 53° 24' longitudes and 31° 11' to 33° 42' latitudes. The annual precipitation varies from 1500 mm in the west to 50 mm in the east of the basin. The Zayandeh-Rud River, with an average natural flow of 1400 million cubic meters (MCM) per year, including 650 MCM of natural flow and 750 MCM of inter-basin transferred flow, starts in the Zagros Mountains in the west of the basin and ends in the Gav Khuni Wetland—a preserved wetland under the Ramsar Convention—in the east of the basin. The Zayandeh Rud River is a vitally important river for agricultural development as well as domestic water supply and economic activity of the Isfahan province in west-central Iran (Safavi et al. 2015). This river passes several agricultural and urban areas, including the populous city of Esfahan—the former capital of Iran. This makes the river the most important water resource of the basin for more than 3.7 million residents and their urban, industrial, and agriculture water consumptions, as well as for the survival of the Gav Khuni Wetland and its valuable ecosystem.

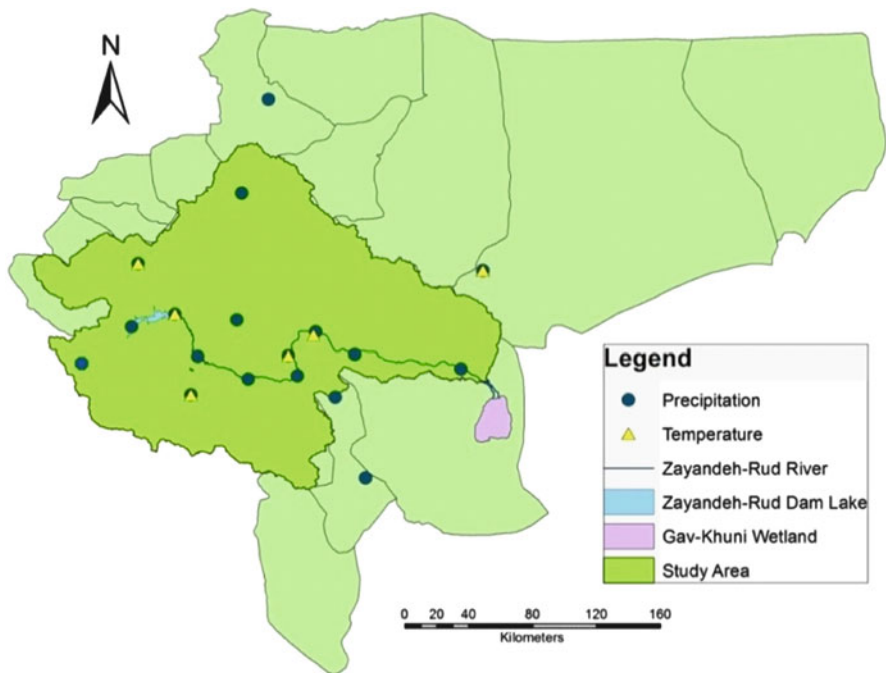


Fig. 13.1 The locations of selected gauges

13.2.1 The Station’s Network in the Study Area

The time series of the climate variables are evaluated based on the time series length and the accuracy of collected climate data while the number of stations is maximized. The doubtful data are removed from the time series and then missing data are generated using WeatherMan software (Hoogenboom et al. 2005). Figure 13.1 shows the locations of the evaporation and rain gauging stations of Energy Ministry in the study area.

At the first step, 100 climatological stations of Energy Ministry are selected. As a 30 year time period (1971–2000) is selected here as a baseline period, the stations with data length less than 30 years are removed.

Therefore, 24 stations including six stations for temperature variable and 18 stations for precipitation are finally considered for this study (Fig. 13.1). Tables 13.1 and 13.2 show the characteristics of the mentioned stations.

Table 13.1 Selected rain gauges in the study area

Station name	Station type	Number of existing record (Years)	Geographic specifications		
			Latitude (Degree)	Longitude (Degree)	Elevation (Meter)
Vežvan Meimeh	Evaporation gauge	45	33.41722	51.18917	2013
Sade Zayandeh Rud	Evaporation gauge	45	32.73417	50.7425	2173
Pol Zamankhan	Evaporation gauge	45	32.49861	50.89528	1880
Zefreh Falavarjan	Evaporation gauge	45	32.50194	51.49861	1648
Damaneh-Feridan	Evaporation gauge	45	33.01833	50.495	2388
Esfahan	Synoptic	49	32.61667	50.495	1550
Mahyar	Evaporation gauge	44	32.26889	51.80889	1686
Fin	Evaporation gauge	42	33.94444	51.37111	1050
Ghaleh Shahrokh	Evaporation gauge	41	32.66278	50.45306	2109
Pol Kaleh	Rain gauge	44	32.37306	51.23056	1771
Ziyar Bravn	Rain gauge	42	32.50611	51.94	1559
Lenj	Rain gauge	45	32.39056	51.55917	1672
Neyestanak Naein	Evaporation gauge	41	32.96806	52.80306	1910
Tiran	Evaporation gauge	45	32.70333	51.15583	1890
Varzaneh	Rain gauge	44	32.41944	52.64694	1495
Maghsoud Beyk	Evaporation gauge	43	31.81278	52.00556	1991
Chelgerd	Rain gauge	47	50.1231	32.4586	2372
Shahrekord	Synoptic	49	32.28333	50.85	2049

13.3 Method

13.3.1 Generation of Climate Change Scenarios

Global Climate Models (GCMs) are considered as the most credible tools for the projections of climate condition and extreme events in the future. In this study, the outputs of 15 GCMs under A2 and B1 emission scenarios from the Fourth Assessment Report (AR4) of Intergovernmental Panel on Climate Change (IPCC) are used (IPCC 2007). The detailed description of the selected models is provided in Table 13.3. The monthly temperature and precipitation data for the baseline period (1971–2000) and future period (2015–2044) are extracted from the Data

Table 13.2 Selected temperature stations in the study area

Station name	Station type	Number of existing record (Years)	Geographic specifications		
			Latitude (Degree)	Longitude (Degree)	Elevation (Meter)
Neyestanak Naein	Evaporation gauge	41	32.968	52.803	1910
Sade Zayandeh Rud	Evaporation gauge	45	32.734	50.742	2173
Falavarjan	Evaporation gauge	38	32.502	51.498	1648
Shahrekord	Synoptic	49	32.283	50.85	2049
Damaneh-Faridan	Evaporation gauge	45	33.018	50.495	2388
Esfahan	Synoptic	49	32.616	50.495	1550

Table 13.3 Description of the 15 GCMs of IPCC's Fourth Assessment Report (AR4)

Model	Abbreviation	Centre
HadCm3	HADCM3	UKMO (UK)
ECHAM5-OM	MPEH5	MPI-M (Germany)
CSIRO-MK3.0	CSMK3	ABM (Australia)
GFDL-CM2.1	GFCM21	NOAA/GFDL (USA)
MRI-CGCM2.3.2	MRCGCM	MRI (Japan)
CCSM3	NCCCSM	NCAR (USA)
CNRM-CM3	CNCM3	CNRM (France)
MIROC3.2	MIMR	NIES (Japan)
IPSL-CM4	IPCM4	IPSL (France)
GISS-E-R	GIER	NASA/GISS (USA)
BCM 2.0	BCM	Beijing Climate Center (China)
CGCM3 T47	CGCM	Canadian Centre for Climate Modelling and Analysis
ECHO-G	ECHO	Meteorological Institute, University of Bonn
INMCM 3.0	INMCM	Russian Academy of Science, Institute of Numerical Mathematics
NCARPCM	NCRPCM	National Center for Atmospheric Research (NCAR), USA

Distribution Centre (DDC) of IPCC. These data are downloaded from the website (<http://www.ccsn.ec.gc.ca>). The differences of the temperature and relative precipitation in the 30 year monthly average future period (2015–2044) and baseline period (1971–2000) are calculated for each month.

13.3.2 The Uncertainty Evaluation of GCMs

There are high levels of uncertainty in outputs of GCMs. These uncertainties affect the confidence in the results of impact assessment studies (Fakhri et al. 2012b). There are many methods for dealing with such uncertainties, including but not limited to expression of the results as a central prediction, a central prediction with error bars, a known probability distribution function, a bounded range with no known probability distribution, and a bounded range within a larger range of unknown probabilities.

13.3.2.1 Weighting the GCMs

Each of the 15 GCMs used in this study is weighted using Eq. (13.1), based on the Mean Observed Temperature–Precipitation (MOTP) method (Massah Bavani and Morid 2005). To weight each model, this method considers the ability of that model in simulating the observed climate variables, i.e., the difference between the simulated average temperature and average precipitation in each month in the baseline period and the corresponding observed values:

$$W_{ij} = \frac{\left(\frac{1}{\Delta_{dij}}\right)}{\sum_j \left(\frac{1}{\Delta_{dij}}\right)} \quad (13.1)$$

where, W_{ij} is the weight of GCM j in month i ; and Δ_{dij} is the difference between average temperature or precipitation simulated by GCM j in month i of base period and the corresponding observed value.

13.3.2.2 Probability Distribution of Temperature and Precipitation Changes

In this step, PDFs of climate change variables are developed for each month. These PDFs relate monthly temperature and precipitation changes to the weight of corresponding GCMs. To evaluate possible effects of climate change, discrete possibilities should be converted to continuous functions. The Beta function was then used to convert discrete probability distributions of change field scenarios to continuous probability distributions: Beta Distribution is defined by parameters of shape, upper and lower data limits. This distribution can be determined by changing shape parameter based on data's skewness. General Form of Beta distribution probability density function is:

$$f(x) = \frac{(x-a)^{p-1} (b-x)^{q-1}}{B(p, q)(b-a)^{p+q-1}} \quad a << x << b; \quad p, q > 0 \quad (13.2)$$

where, p and q are the shape parameters, a and b are respectively the upper and lower data limits and $B(p, q)$ is the Beta function. Therefore, the Beta distribution is fitted to climate change scenarios of precipitation, minimum and maximum temperature for each month.

In this part, on the basis of fitted Beta distribution functions, Cumulative Distribution Function (CDF) curve of temperature and precipitation changes of being equal to or more than the base generated for each month. Monthly ΔT and ΔP values for 50% probability level have been extracted from the CDF curves. Selected possibility level indicates an average climate condition during the future periods.

13.3.2.3 Downscaling

Low spatial resolution of models and great uncertainty in their daily outputs, especially for precipitation, result in the output that is not proper for direct use in simulating models stages and analysis of severe events. The downscaling techniques are used to bridge the gap between the GCMs' outputs and required inputs of impacts assessment models (Rajabi et al. 2010). Stochastic Weather Generator is one of statistical downscaling methods for creating daily weather scenarios in a specific station. LARS-WG is here used to generate future daily time series of maximum and minimum temperatures and precipitation under climate change scenarios.

13.3.3 Regionalization

13.3.3.1 Regionalization of Downscaled Precipitation

As the results of this study are planning to apply for the simulation of the hydrologic conditions of the Zayandeh-Rud River Basin under climate change, the climate change scenarios for 58 stations should be projected as the imputes for hydrologic model. Therefore the results of climate change in 18 stations had to be regionalized to project the climate change scenarios for all required stations (58 stations) for the hydrologic model (Fig. 13.2).

As precipitation has considerable variations in the study area, daily precipitation correlation of each of remaining stations (40 stations) with the climate change study stations (18 stations) during their available data period are calculated in order to predict the precipitation values. Four different methods including Inverse Distance Weighting, Kriging, Natural Neighbourhood and Spline are applied for regionalization. In the next step, historical daily records of four stations, named Dezak Abad

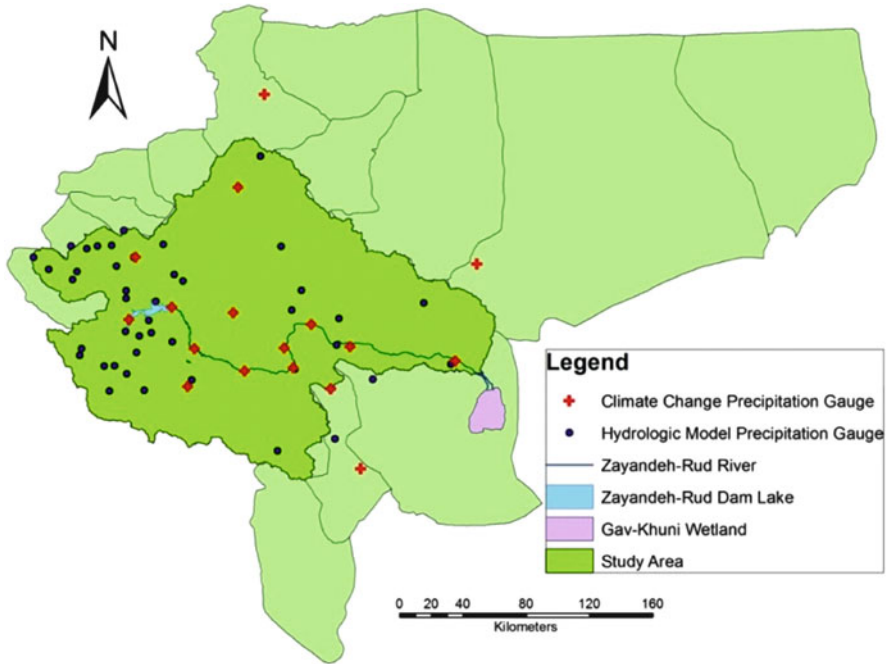


Fig. 13.2 Situation of both climate change and hydrologic model precipitation stations

and Boein located in upstream of study area and Kouhpaye and Mohammad-Abad-Jarghoye in downstream, are constructed by these four methods and compared with the observation data to compare the accuracy of the mentioned methods.

According to the better coincidence of Natural Neighbourhood predicted quantities, this method is used for the regionalization of precipitation. Comparison of the results is shown in the Table 13.4.

13.3.3.2 Regionalization of Downscaled Temperature

The six selected temperature stations is used for regionalization of temperature variables for 25 stations needed for hydrologic model. Spatial distribution of stations is shown in Fig. 13.3. Three temperature stations named Ghale Shahrokh, Kouhpaye and Morche-Khort are used to select the appropriate method for the regionalisation of temperature. Daily quantities of temperature for the three stations are interpolated by using IDW, Kriging and Natural Neighbourhood and compared with historical observations. Comparison of the results is mentioned in Table 13.5. The results showed the IDW can have acceptable capability in the regionalisation of temperature in this study.

Table 13.4 Comparison of the results of interpolation methods for aforementioned stations (in millimetres)

Station	Interpolation method	RMSE	R ²	Yearly mean precipitation (Estimated)	Yearly mean precipitation (Observed)
Boein	IDW	2.63	0.66	387	321
	Kriging	2.71	0.64	394	
	Natural Neighbourhood	2.57	0.66	371	
	SPLine	2.73	0.66	373	
Dezak Abad	IDW	5.85	0.67	1094	859
	Kriging	5.23	0.68	951	
	Natural Neighbourhood	5.64	0.67	1043	
	SPLine	5.97	0.67	1111	
Kouhpaye	IDW	1.36	0.51	143	112
	Kriging	1.36	0.51	143	
	Natural Neighbourhood	1.25	0.52	122	
	SPLine	1.42	0.5	145	
Mohamad-Abad-Jarghouye	IDW	1.23	0.59	137	96
	Kriging	1.12	0.64	131	
	Natural Neighbourhood	1.08	0.64	125	
	SPLine	1.27	0.58	138	

13.4 Results and Discussion

Figures 13.4 and 13.5 show the average of temperature changes in all weather stations for the A2 and B1 emission scenarios. These values are obtained by 30 year averaging of temperature in six weather stations for each month. Also, in this Figure, the spatial variability in temperature changes has been shown by vertical lines. The average temperature during all months is increased for all emission scenarios, though this increase is varied in different months. The maximum increase in temperature is observed in September. The minimum temperature increase occurs in January, though this is less in the initial months of the years.

Seasonal and annual changes of temperature in the Zayandeh-Rud River Basin have been summarized in Tables 13.6 and 13.7. The results show that optimistically, annual temperature in the Zayandeh-Rud River Basin will be increased by 0.6–1.1 °C in different weather stations. Summer will experience the maximum increase in temperature in all weather stations and for both emission scenarios. Winter will also have the minimum temperature increase. Overall, the A2 emission scenario shows more temperature increase in comparison with the B1 emission scenario.

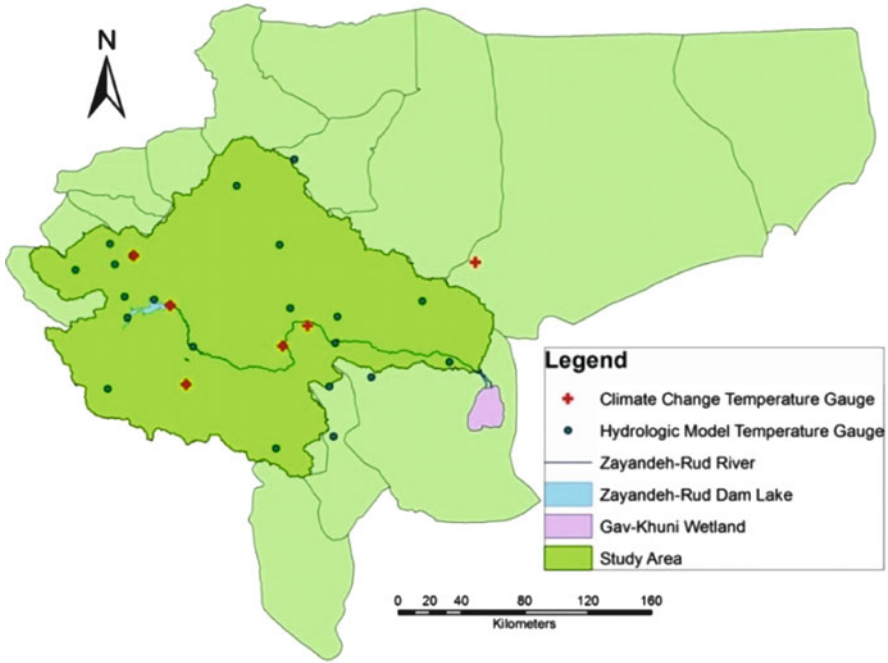


Fig. 13.3 Distribution of temperature stations for climate change and hydrologic model

Table 13.5 Comparison of the results interpolation methods for temperature in different stations

Station	Method	R2	
		Min. temp.	Max. temp.
Ghale Shahrokh	IDW	0.87	0.88
	Kriging	0.86	0.87
	Natural Neighborhood	0.87	0.88
Kouhpaye	IDW	0.9	0.93
	Kriging	0.88	0.92
	Natural Neighborhood	0.9	0.91
Morche-Khort	IDW	0.93	0.87
	Kriging	0.92	0.87
	Natural Neighborhood	0.93	0.87

Growing warming for Middle East regions is predicted by several studies using climate change indices which primarily focus on extremes (Alexander et al. 2006; Sensoy et al. 2007; Lelieveld et al. 2012). The relatively strong upward trend of temperature in the northern regions of the East Mediterranean and the Middle East indicates a continuation of the increasing intensity and duration of heat waves observed in this region since 1960 (Kuglitsch et al. 2010). Later studies also show a decrease in precipitation and increase in extreme precipitation for some

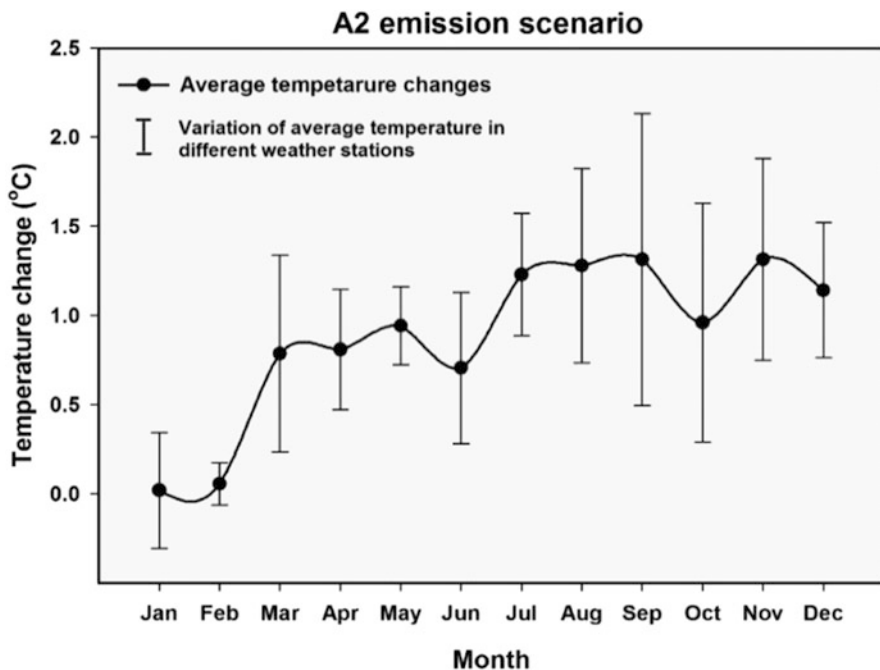


Fig. 13.4 Average monthly temperature change in different weather stations for A2 emission scenario

regions in Middle East and have a good consistency with results of current study. However, the modelled changes in precipitation exhibit a large variability in space and time and there is a less spatially coherent pattern of change and a lower level of statistical significance for precipitation compared with temperature changes.

Figures 13.6 and 13.7 show the average of precipitation changes in 18 weather stations for different emission scenarios. These values are obtained based on the 30 year averaging of precipitation predicted in each month. Also, the spatial variability of the precipitation has been shown by vertical lines. The amount of precipitation changes don't follow a uniform increasing or decreasing trend. However, in cold months (January, February and March), precipitation always decreases for A2 and B1 emission scenarios. In other hand, precipitation in future warm months is increased for all emission scenarios. However, the most precipitation in the Zayandeh-Rud River Basin occurs in the cold months.

Seasonal and annual precipitation variations in all weather stations have been shown in Table 13.8. Winter is found to have the maximum precipitation decrease in comparison with other seasons. As in 1971–2000, summer had very low precipitation, the precipitation changes rainfall in this season are negligible and had the minimum precipitation changes in A2 and B1 emission scenarios.

Comparison of annual precipitation in the near future shows that precipitation will be changed from -0.53 to $+0.42\%$ in all weather stations. Overall, the A2

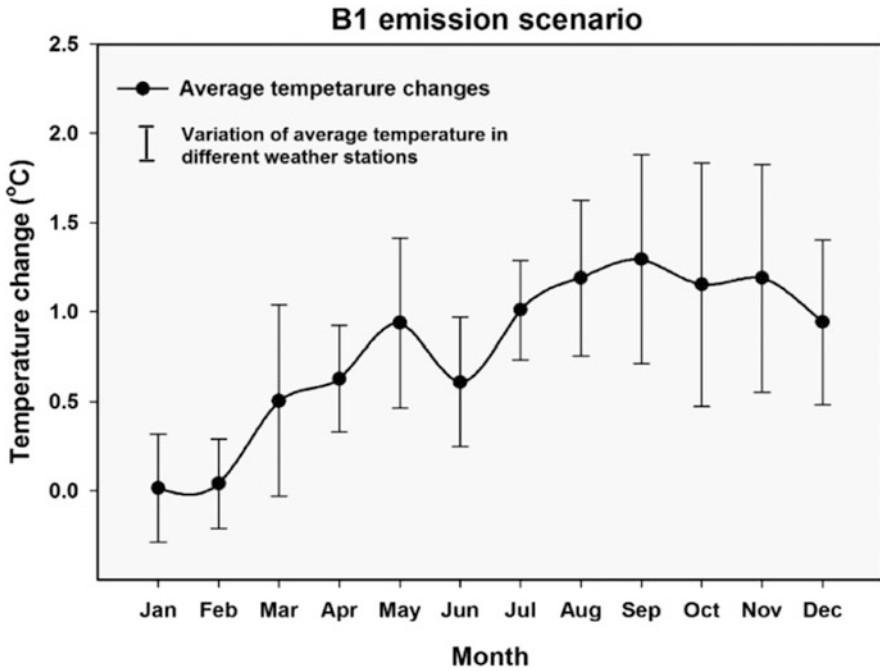


Fig. 13.5 Average monthly temperature change in different weather stations for B1 emission scenario

Table 13.6 Seasonal and annual temperature changes in different weather stations for A2 emission scenario

Month	Temperature changes (°C)					
	Neyestanak	Falavarjan	Sade Zayandeh Rud	Esfahan	Damaneh	Shahrekord
Winter	-0.2	0.4	0.5	0.4	0.4	0.3
Spring	0.3	1.0	1.0	0.8	0.7	1.0
Summer	2.0	1.1	1.4	1.4	0.6	1.0
Fall	1.9	1.1	1.3	1.2	0.6	0.9
Annual	1.0	0.9	1.1	1.0	0.6	0.8

emission scenario shows more annual precipitation decrease than the B1 emission in all weather stations.

Yearly average of baseline period precipitation, as shown in Fig. 13.8, has a high variation from the extreme value of 1450 mm/year in the west to the lowest value of 85 mm/year in the east. Meanwhile, yearly average of precipitation under A2 (B1) scenario, has predicted a decline in the region as much as 26% (27%) in the west and 7% (2%) in the east. This resulted in precipitation range fall to 1063 (1053) and 79 (83) mm/year. The gradient of precipitation changes decreased under both scenarios.

Table 13.7 Seasonal and annual temperature changes in different weather stations for B1 emission scenario

Month	Temperature changes (°C)					
	Neyestanak	Falavarjan	Sade Zayandeh-Rud	Esfahan	Damaneh	Shahrekord
Winter	-0.6	0.2	0.3	0.3	0.3	0.2
Spring	0.1	0.9	1.0	0.7	0.7	0.9
Summer	1.8	1.0	1.1	1.1	0.8	1.2
Fall	1.7	1.1	0.8	1.0	0.5	0.8
Annual	0.9	0.8	0.8	0.8	0.6	0.8

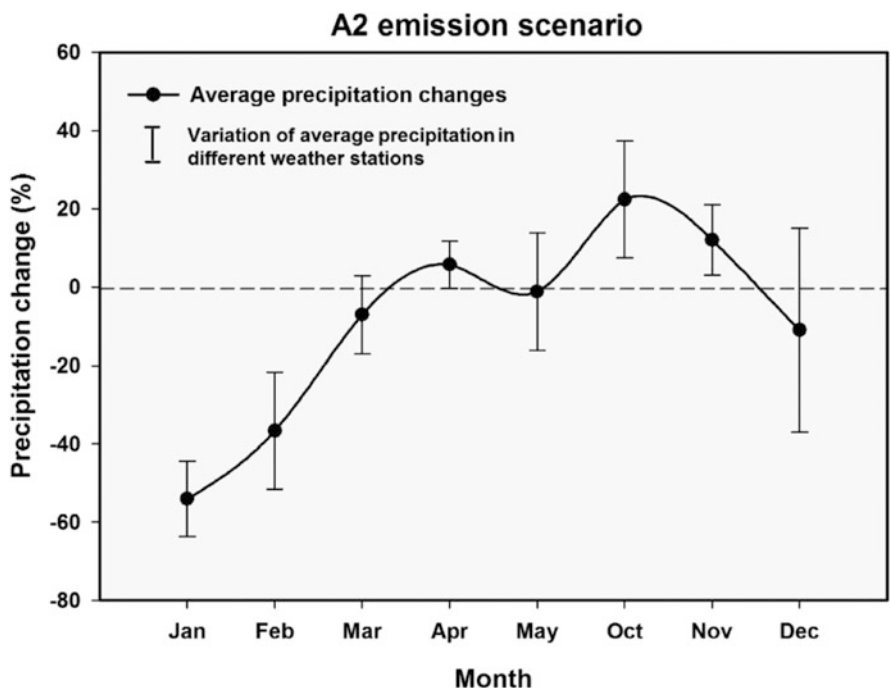


Fig. 13.6 Average monthly precipitation change in different weather stations for A2 emission scenario

Baseline mean temperature yearly average is depicted in Fig. 13.9. Low value of 9.7 °C in the west higher altitudes increases gradually to value of 16.3 °C in the east within the lowest altitudes. Under A2 (B1) scenario, it is predicted to vary temperature range of study area to 10.3–16.8 °C (10.3–16.6 °C). This means an increase of 6.2% and 3% (6.2% and 1.8%) in lower and upper bounds of temperature range, respectively. It can be seen that B1 scenario predicted intensification in gradient of variations of temperature in the study area. Central warmer region of study area has been extended to more areas under both scenarios.

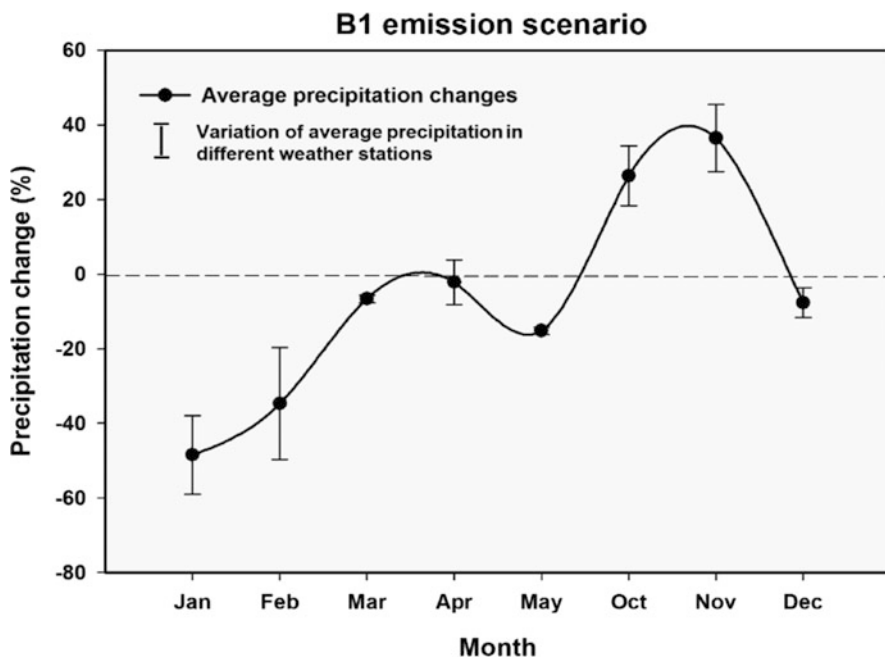


Fig. 13.7 Average monthly precipitation change in different weather stations for B1 emission scenario

Table 13.8 Seasonal and annual temperature changes in different weather stations for different emission scenarios

Weather station	A2 emission scenario				B1 emission scenario			
	Winter	Spring	Fall	Annual	Winter	Spring	Fall	Annual
Esfahan	-0.30	0.11	-0.24	-0.14	-0.26	0.14	-0.01	-0.04
Pol Zamankhan	-0.45	-0.09	0.66	0.04	-0.41	0.03	0.42	0.01
Pol Kale	-0.34	0.02	0.12	-0.07	-0.14	-0.20	0.21	-0.04
Chelgerd	-0.45	-0.03	-0.19	-0.22	-0.43	0.07	-0.23	-0.20
Damaneh	-0.31	0.16	0.13	-0.01	-0.23	0.06	0.03	-0.05
Sad Zayandeh Rud	-0.31	0.40	0.10	0.06	-0.33	-0.41	0.28	-0.15
Falavarjan	-0.50	0.06	-0.26	-0.24	-0.53	-0.30	0.28	-0.18
Ghale Shahrokh	-0.31	0.11	0.08	-0.04	-0.32	-0.05	0.25	-0.04
Lenj	-0.15	0.03	0.49	0.12	-0.18	0.01	0.30	0.04
Maghsoud Beik	-0.26	-0.18	0.18	-0.09	-0.21	-0.24	0.29	-0.05
Mahyar	-0.18	-0.19	0.09	-0.09	-0.23	-0.03	0.30	0.02
Neyestanak	-0.18	-0.19	0.09	-0.09	-0.37	0.08	-0.41	-0.23
Falavarjan	-0.51	0.06	-0.26	-0.24	-0.53	-0.29	0.28	-0.18
Shaherekord	-0.48	0.14	0.23	-0.04	-0.29	-0.05	0.27	-0.03
Fin	-0.30	-0.07	0.17	-0.07	-0.26	0.04	0.12	-0.03
Vezvan	-0.31	0.04	-0.15	-0.14	-0.22	-0.16	0.32	-0.02
Varzaneh	-0.20	0.03	0.11	-0.02	-0.16	-0.18	0.42	0.03

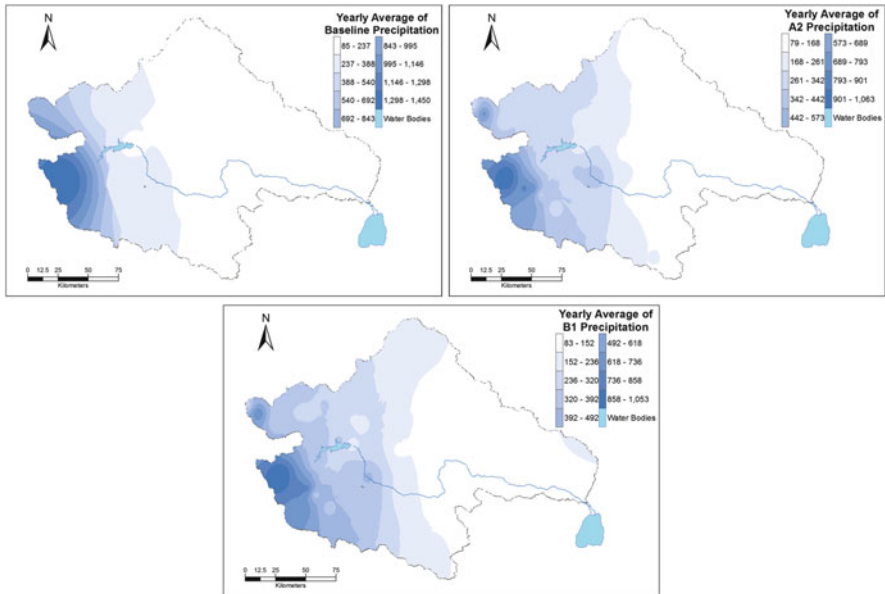


Fig. 13.8 Yearly average of baseline period, A2 and B1 precipitation

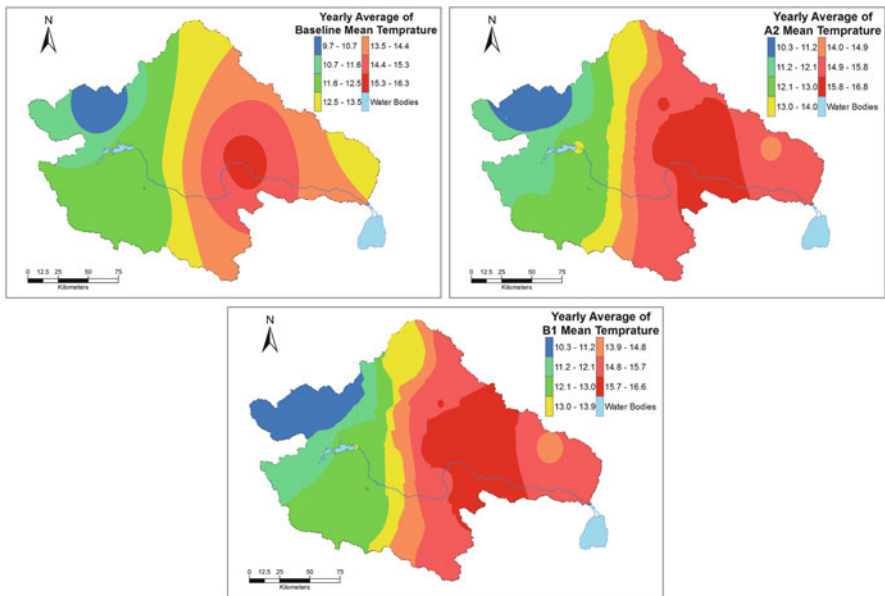


Fig. 13.9 Yearly average of baseline period, A2 and B1 mean temperature

13.5 Conclusions

Analysis of climate change impacts on the temperature indicates an increase pattern in temperature in all stations under study. General increasing trend of temperature in the upstream and downstream stations shows the lowest values of temperature increase simulated in the winter while the highest temperature increase values will be in spring and summer.

For stations in upper regions of the basin, the highest values of increase in temperature are expected in spring months. The increasing trend of winter temperature in the upper sub-basin stations can affect the amounts of snowfall and precipitation falls as rain than snow, leading to the reduction in the volume of snow pack. Generally, temperature change shows an increasing trend from the West to East and has an inverse relationship with the height.

Results of climate change impacts on the precipitation in Chelgerd station located in upstream of basin show the highest quantities of precipitation decrease at annual scale. As far as the quantities of precipitation in this region can influence considerably Zayandeh-Rud river flow, it is predicted that 25–26% reduction of annual precipitation in this area will have considerable effects on the natural river flow during the study years. The seasonal results of precipitation shows its patterns change from winter to spring and fall seasons in up- and down-stream of Zayandeh-Rud basin. In a general view, precipitation changes show a decreasing trend from the West to East and it has a direct relationship with height.

References

- Alexander LV, Zhang X, Peterson TC, Caesar J, Gleason B, Klein Tank AMG, Tagipour A (2006) Global observed changes in daily climate extremes of temperature and precipitation. *J Geophys Res Atmos* 111(D5). doi:[10.1029/2005JD006290](https://doi.org/10.1029/2005JD006290)
- Barnett TP, Adam JC, Lettenmaier DP (2005) Potential impacts of a warming climate on water availability in snow-dominated regions. *Nature* 438(7066):303–309
- Bates B, Kundzewicz ZW, Wu S, Palutikof J (2008) Climate change and water: Technical paper VI. Intergovernmental Panel on Climate Change (IPCC)
- Betts RA (2005) Integrated approaches to climate–crop modelling: needs and challenges. *Philos Trans R Soc Lond Ser B Biol Sci* 360(1463):2049–2065
- Bradley RS, Vuille M, Diaz HF, Vergara W (2006) Threats to water supplies in the tropical Andes. *Science* 312:1755–1756
- Daccache A, Weatherhead EK, Stalham MA, Knox JW (2011) Impacts of climate change on irrigated potato production in a humid climate. *Agric For Meteorol* 151(12):1641–1653
- Dawson B, Spannagle M (2009) The complete guide to climate change. Routledge, New York, NY
- Diaz HF, Grosjean M, Graumlich L (2003) Climate variability and change in high elevation regions: past, present and future. *Clim Chang* 59:1–4
- Douville H, Chauvin F, Planton S, Royer JF, Salas-Melia D, Tyteca S (2002) Sensitivity of the hydrological cycle to increasing amounts of greenhouse gases and aerosols. *Clim Dyn* 20(1):45–68
- Elmahdi A (2008) WBFS model: strategic water and food security planning on national wide level. IGU-2008 Water Sustainability Commission, Tunis

- Eslamian SS, Khordadi MJ, Abedi-Koupai J (2011) Effects of variations in climatic parameters on evapotranspiration in the arid and semi-arid regions. *Glob Planet Chang* 78:188–194
- Fakhri M, Farzaneh MR, Eslamian S, Khordadi MJ (2012a) Uncertainty assessment of downscaled rainfall: impact of climate change on the probability of flood. *J Flood Eng* 3(1):19–28
- Fakhri M, Farzaneh MR, Eslamian SS, Khordadi MJ (2012b) Confidence interval assessment to estimate dry and wet spells under climate change in Shahrekord station, Iran, ASCE. *J Hydrol Eng* 18(7):911–918
- Gohari A, Eslamian S, Abedi-Koupai J, Massah-Bavani A, Wang D, Madani K (2013) Climate change impacts on crop production in Iran's Zayandeh-Rud River Basin. *Sci Total Environ* 442:405–419
- Hoogenboom G, Jones JW, Wilkens PW, Porter CH, Hunt LA, Boote KJ, Singh U, Uryasev O, Lizaso JI, Gijssman AJ, White JW, Batchelor WD, Tsuji GY (2005) Decision support system for agrotechnology transfer, *Weatherman*. Release 4.0.2.0. University of Hawaii, Honolulu, HI
- Huber U, Reasoner M, Bugmann H (eds) (2005) *Global change and mountain regions, a state of knowledge overview*. Kluwer Academic Publishers, Dordrecht, 652 pp
- IPCC (2007) *General guidelines on the use of scenario data for climate impact and adaptation assessment*. Cambridge University Press, Cambridge/New York
- Khan MS, Coulbaly P, Dibike Y (2006) Uncertainty analysis of statistical downscaling methods. *J Hydrol* 319(1):357–382
- Kuglitsch FG, Toreti A, Xoplaki E, Della Marta PM, Zerefos CS, Türkeş M, Luterbacher J (2010) Heat wave changes in the eastern Mediterranean since 1960. *Geophys Res Lett* 37:L04802. doi:[10.1029/2009GL041841](https://doi.org/10.1029/2009GL041841)
- Lelieveld J, Hadjinicolaou P, Kostopoulou E, Chenoweth J, El Maayar M, Giannakopoulos C, Xoplaki E (2012) Climate change and impacts in the Eastern Mediterranean and the Middle East. *Clim Chang* 114(3–4):667–687
- Madani K, Marino MA (2009) System dynamics analysis for managing Iran's Zayandeh-Rud River Basin. *Water Resour Manag* 23:2163–2187
- Massah Bavani AR, Morid S (2005) The impacts of climate change on water resources and agricultural production. *J Water Resour Res* 1:40–47. (In Persian)
- Nogués-Bravo D, Araújo MB, Errea MP, Martínez-Rica JP (2007) Exposure of global mountain systems to climate warming during the 21st Century. *Glob Environ Chang* 17(3):420–428
- Parry ML, Rosenzweig C, Iglesias A, Livermore M, Fischer G (2004) Effects of climate change on global food production under SRES emissions and socio-economic scenarios. *Glob Environ Chang* 14(1):53–67
- Prudhomme C, Jakob D, Svensson C (2003) Uncertainty and climate change impact on the flood regime of small UK catchments. *J Hydrol* 277:1–23
- Rajabi A, Sedghi H, Eslamian SS, Musavi H (2010) Comparison of Lars-WG and SDSM downscaling models in Kermanshah (Iran). *Ecol Environ Conserv* 16(4):1–7
- Safavi HR, Golmohammadi MH, Sandoval-Solis S (2015) Expert knowledge based modeling for integrated water resources planning and management in the Zayandehrud River Basin. *J Hydrol* 528:773–789
- Sensy S, Peterson TC, Alexander LV, Zhang X (2007) Enhancing Middle East climate change monitoring and indexes. *Bull Am Meteorol Soc* 88(8):1249
- Sorg A, Bolch T, Stoffel M, Solomina O, Beniston M (2012) Climate change impacts on glaciers and runoff in Tien Shan (Central Asia). *Nat Clim Chang* 2(10):725–731
- Tao F, Zhang Z (2010) Adaptation of maize production to climate change in North China Plain: quantify the relative contributions of adaptation options. *Eur J Agron* 33(2):103–116
- Tao F, Yokozawa M, Zhang Z (2009) Modelling the impacts of weather and climate variability on crop productivity over a large area: a new process-based model development, optimization, and uncertainties analysis. *Agric For Meteorol* 149(5):831–850